Molecular Plant • Volume 5 • Number 5 • Pages 1100–1112 • September 2012 RESEARCH ARTICLE

Map-Based Cloning of *zb7* Encoding an IPP and DMAPP Synthase in the MEP Pathway of Maize

Xiao-Min Lu[a,b,2], Xiao-Jiao Hu[a,2], Yuan-Zeng Zhao[a,c,2], Wei-Bin Song[a], Mei Zhang[a], Zong-Liang Chen[a], Wei Chen[a], Yong-Bin Dong[a], Zhen-Hua Wang[b] and **Jin-Sheng Lai[a,1]**

a State Key Laboratory of Agrobiotechnology and National Maize Improvement Center, Department of Plant Genetics and Breeding, China Agricultural University, Beijing, 100193, PR China
b Henan Academy of Agricultural Science, Zhengzhou, 450002, PR China
c Department of Life Science and Technology, Henan Institute of Science and Technology, Xinxiang 453003, PR China

ABSTRACT IspH is a key enzyme in the last step of the methyl-D-erythritol-4-phosphate (MEP) pathway. Loss of function of IspH can often result in complete yellow or albino phenotype in many plants. Here, we report the characterization of a recessive mutant of maize, *zebra7 (zb7),* showing transverse green/yellow striped leaves in young plants. The yellow bands of the mutant have decreased levels of chlorophylls and carotenoids with delayed chloroplast development. Low temperature suppressed mutant phenotype, while alternate light/dark cycle or high temperature enlarged the yellow section. Map-based cloning demonstrated that *zb7* encodes the IspH protein with a mis-sense mutation in a conserved region. Transgenic silencing of *Zb7* in maize resulted in complete albino plantlets that are aborted in a few weeks, confirming that *Zb7* is important in the early stages of maize chloroplast development. *Zb7* is constitutively expressed and its expression subject to a 16-h light/8-h dark cycle regulation. Our results suggest that the less effective or unstable IspH in *zb7* mutant, together with its diurnal expression, are mechanistically accounted for the zebra phenotype. The increased IspH mRNA in the leaves of *zb7* at the late development stage may explain the restoration of mutant phenotype in mature stages.

Key words: *zb7* mutant; chloroplast; IspH; RNAi; map-based cloning.

INTRODUCTION

Isoprenoids play essential roles in plant growth and development. In higher plants, biosynthesis of the basic isoprenoid units occurs by two different pathways: the mevalonate (MVA) pathway and the methyl-D-erythritol-4-phosphate (MEP) pathway (Supplemental Figure 1). For decades, it was thought that the MVA pathway was solely responsible for isoprenoid biosynthesis. However, the alternative MEP pathway was discovered recently in bacteria, green algae, and higher plants (Rohmer et al., 1993; Eisenreich et al., 1998; Lichtenthaler, 1999; Cunningham Jr et al., 2000; Rodríguez-Concepción and Boronat, 2002; Rohmer, 2003). The MVA pathway occurs in the cytosol and is responsible for the synthesis of sterols, certain sesquiterpenes, and the side chain of ubiquinone (Disch et al., 1998). By contrast, the MEP pathway operates in the plastids and is involved in providing the precursors for monoterpenes, isoprene, chlorophylls, carotenoids, tocopherols, taxadiene, gibberellins, and abscisic acid (Schwender et al., 1996; Zeidler et al., 1997; Eisenreich et al., 1998; Lichtenthaler, 1999; Rohmer, 1999) (Supplemental Figure 1). In recent years, the entire MEP pathway and almost all the enzymes involved have been identified in *Escherichia coli*. The activity of the corresponding enzyme and the roles they played in the pathway have been widely demonstrated (Sprenger et al., 1997; Lois et al., 1998; Takahashi et al., 1998; Rohdich et al., 1999; Herz et al., 2000; Lüttgen et al., 2000; Hecht et al., 2001; Adam et al., 2002). The genes encoding each enzyme in the MEP pathway are highly conserved.

Genes encoding enzymes involved in the MEP pathway are important for chlorophyll and carotenoid biosynthesis in plants. Knockout mutations of several genes in this pathway in *Arabidopsis* and *Nicotiana benthamiana* display albino phenotype (Mandel et al., 1996; Araki et al., 2000; Estévez et al., 2000; Budziszewski et al., 2001; Gutiérrez-Nava et al., 2004; Page et al., 2004; Guevara-García et al., 2005). The transcript accumulation is modulated by multiple external signals, such as light, nutritional cues. Posttranscriptional regulation of

[1] To whom correspondence should be addressed. E-mail jlai@cau.edu.cn.

[2] These authors contributed equally to this study.

doi: 10.1093/mp/sss038, Advance access publication 12 April 2012
Received 14 November 2011; accepted 2 March 2012

some enzymes of the MEP pathway has also been detected (Carretero-Paulet et al., 2002; Guevara-García et al., 2005; Hsieh and Goodman, 2005; Hsieh et al., 2008).

IspH (also called HDR or LytB) catalyzes the last step of the MEP pathway and plays a rate-limiting role in the pathway. It was originally characterized in *E. coli* during studies of penicillin tolerance and the control of the stringent response (Gustafson et al., 1993). Since then, molecular studies of the *IspH* gene have been performed in different organisms and during different developmental stages. Mutagenesis studies in *E. coli* suggested that the *IspH* gene is essential, as it is responsible for producing a metabolite required for isoprenoid biosynthesis in the non-MVA pathway (Altincicek et al., 2001; McAteer et al., 2001). In the leaves of *Nicotiana benthamiana*, down-regulation of the *IspH* gene by virus-induced gene silencing results in albino phenotype (Page et al., 2004). Analyses of *HDR* expression in tomato fruit ripening and *A. thaliana* seedling de-etiolation demonstrated that *HDR* is important in regulating the production of precursors for carotenoid and taxadiene biosyntheses (Botella Pavía et al., 2004). Studies on a collection of characterized *A. thaliana* chloroplast biogenesis albino mutants revealed that *clb6* mutants are caused by loss of function of the *IspH* gene (Gutiérrez-Nava et al., 2004; Guevara-García et al., 2005). Characterization of the *clb6* mutant and the null mutation in *A. thaliana* illustrated that IspH is posttranscriptionally regulated and that it is coordinately regulated under a 16-h light/8-h dark cycle (Guevara-García et al., 2005; Hsieh and Goodman, 2005). Recently, *in vivo* Mossbauer Spectroscopy of the LytB protein indicated that it contains an unusual $[4Fe\text{-}4S]^{2+}$ cluster that is attached to the protein by three conserved cysteine residues. This cluster contains a hexacoordinated iron linked to three of the sulfurs and three additional oxygen and nitrogen ligands (Seemann et al., 2009).

Single-recessive mutations that cause variegated or striped patterns are known in many species, including maize, rice, barley, and *Arabidopsis* (Hansson et al., 1997; Aluru et al., 2001; Huang et al., 2009; Chai et al., 2011). The leaves of these mutants have green and yellow (or white) sections. The yellow/white sections of the mutant contain decreased levels of chlorophylls and carotenoids and show impaired chloroplast structure. The variegated mutant usually has enhanced sensitive to environmental factors, such as temperature and light. Recent cloning of the responsible genes has indicated that leaf variegation occurs through various metabolic pathways. *Arabidopsis im*, which exhibits light-dependent leaf variegation, is a classic example of variegation. The responsible gene *IMMUTANS* encodes a chloroplast terminal oxidase and functions in phytoene desaturation during carotenoid biosynthesis (Carol et al., 1999; Carol and Kuntz, 2001). Rice *zebra2-1* mutant was caused by the mutation in carotenoid isomerase (Chai et al., 2011). Inactivation of *ZEBRA2* causes a decrease in carotenoids content followed by the accumulation of ROS that results in photoinhibition and photobleaching (Chai et al., 2011). Maize *camouflage1* (*cf1*) mutant develops nonclonal, yellow–green sectors in its leaves. The *cf1* gene encodes porphobilinogen deaminase (PBGD), an enzyme that functions early in chlorophyll and heme biosynthesis. A threshold model is discussed that incorporates photosynthetic cell differentiation and the roles of light and ROS homeostasis (Huang et al., 2009).

In this study, a maize recessive mutant, *zebra7* (*zb7*), is characterized. The seedling of the mutant exhibits a transverse yellow–green strip leaf phenotype. Additionally, we determined that expression of *zb7* phenotype was affected by the light/dark cycle and temperature. Map-based cloning demonstrated that *zb7* is a mis-sense mutation (C to T at residue 190, which results in an amino acid change of Arg to Cys at position 64) of IspH. Gene silencing of IspH in maize resulting in albino phenotype confirmed that IspH is essential in the early stages of chloroplast development in maize. Our results suggest that the phenotype of transverse green/yellow stripes on the mutant leaves is due to the less effective or unstable mutant IspH protein and its diurnal expression. Our result also indicates that the higher expression level of mutated IspH at mature stage may explain the restoration of mutant phenotype.

RESULTS

Phenotypic Characterization of the *zb7* Mutant

The *zb7* mutant exhibited transverse yellow–green crossbands leaf phenotype in its seedling stage (Figure 1B). Under normal conditions, the yellow–green crossbands gradually disappeared after the 10-leaf stage (Supplemental Figure 2). The *zb7* mutant was slightly smaller than the wild-type at the three-leaf stage and had reduced cell contents of chlorophyll a (Chl a), chlorophyll b (Chl b), and carotenoids throughout development (Table 1). At the three-leaf stage, the yellow bands of the *zb7* contained significantly lower levels of Chl a, Chl b, and carotenoids compared to those in the *zb7*-green sections and the wild-type plant. Pigment levels in *zb7* yellow sectors were decreased to approximately 44–62% compared to wild-type (Table 1). At the nine-leaf stage, levels of Chl a, Chl b, and carotenoids were still lower in the yellow bands of the mutant compared to those in green sections and the wild-type plant (Table 1). Once the yellow–green crossbands had disappeared (i.e. when the plants reached adult stage and had turned completely green), the pigment contents of the *zb7* mutant are similar to the wild-type (Table 1).

To investigate the effects of the *zb7* mutation on the ultrastructure of chloroplasts, leaf sections from wild-type, *zb7*-green, and *zb7*-yellow plants at different stages of development were analyzed by transmission electron microscopy (TEM) (Figure 1). The leaf cells of B73 possessed both normal and abnormal chloroplasts (Figure 1H). In the cells from the green sections of the mutant leaves, most of the chloroplasts were normal but appeared to contain fewer grana stacks compared to the wild-type (Figure 1I). In contrast, in the yellow sections, the internal structures of the chloroplasts were

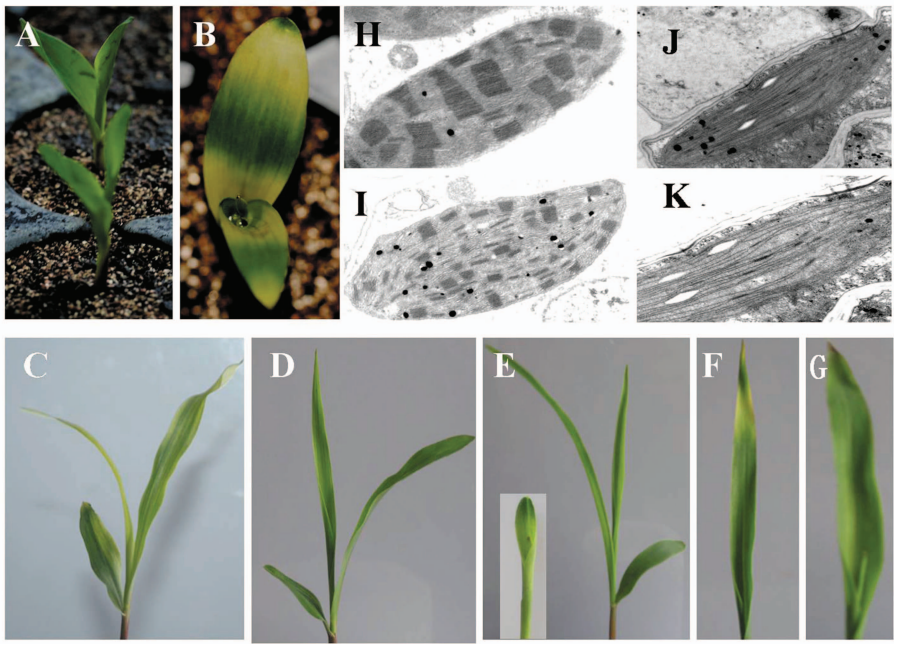

Figure 1. The Performance of *zb7* Mutant at Different Light and Temperature Regimens and Chloroplast Ultrastructures from Wild-Type and *zb7* Mutant Plants.

(A) Wild-type.
(B) 16-h light at 32°C/8-h dark at 22°C, or 16-h light/8-h dark at 28°C, or 16-h light/8-h dark at 32°C, or 24-h light with 16-h at 32°C/8-h at 22°C or 24-h light, at 22°C
(C) 24-h light, at 32°C.
(D) 16-h light/8-h dark at 18°C or 24-h light at 18°C.
(E) 16-h light/8-h dark at 22°C.
(F) First 16-h at 32°C/8-h dark at 22°C, later 24-h light, 18°C after two-leaf stage.
(G) 16-h at 32°C/8-h dark at 22°C after (F).
(H) Normal chloroplast ultrastructure with well-ordered and abundant stacks in B73.
(I) Basic normal chloroplast with fewer granal stacks in *zb7*-green cells.
(J) Disordered grana and decomposition of grana stacks in *zb7*-yellow cells.
(K) Ampliate two multiple image of J. Bar equals 0.5 μm.

severely disaggregated and contained vesicle structures with high electron density (Figures 1J and 1K).

Light and Temperature Conditions Affect the Zebra Phenotype

Previous reports showed that many variegation mutants are light and/or temperature sensitive (Carol et al., 1999; Kusumi et al., 2000; Aluru et al., 2001; Carol and Kuntz, 2001). To test this, *zb7* mutants were grown at 10 different light and temperature regimens to determine the effects of light and temperature on the zebra crossbands phenotype: (1) 18°C, 16-h light/8-h dark; (2) 22°C, 16-h light/8-h dark; (3) 28°C, 16-h light/8-h dark; (4) 32°C, 16-h light/8-h dark; (5) 16 h at 32°C/8 h at 22°C, 24-h light; (6) 32°C, 24-h light; (7) 22°C, 24-h light; (8) 16-h light at 32°C/8-h dark at 22°C; (9) 18°C after 5-d germination as regimen 8; (10) regimen 8 after regimen 9. All the plants were germinated so as to provide mutant seedlings at the three-to-four-leaf stage. The *zb7* mutant showed obvious horizontal zebra crossbands when grown under regimens 3, 4, 5, 7, and 8 (Figure 1B). Seedlings under regimen 1 were totally green (Figure 1D). Under regimen 2, the seedlings showed slight alternating yellow–green cross-bands on the young shoots but they soon turned completely

Table 1. Content of Photosynthetic Pigments in Leaves of Wild-Type and *zb7* Mutant Plants.

Growth stage	Genotype	Total Chl a	Chl b	Car
Three-leaf	Wild-type	1.08 ± 0.08	0.39 ± 0.08	0.23 ± 0.02
Three-leaf	*zb7* green	1.18 ± 0.27	0.39 ± 0.12	0.24 ± 0.04
Three-leaf	zb7 yellow	0.48 ± 0.16	0.24 ± 0.07	0.10 ± 0.04
Nine-leaf	Wild-type	1.39 ± 0.16	0.68 ± 0.35	0.35 ± 0.09
Nine-leaf	zb7 green	1.60 ± 0.10	0.57 ± 0.10	0.34 ± 0.04
Nine-leaf	zb7 yellow	1.07 ± 0.07	0.38 ± 0.07	0.27 ± 0.02
Adult	Wild-type	2.32 ± 0.03	0.99 ± 0.02	0.37 ± 0.01
Adult	zb7	2.29 ± 0.12	0.93 ± 0.13	0.37 ± 0.01

Chlorophylls and carotenoids were measured in acetone extracts from the second leaf from the top of plants in different growth stages. Values are mg g^{-1} fresh weight and are given as the mean (±1 standard deviation) of five independent determinations.

green (Figure 1E). Surprisingly, the three-leaf stage of the *zb7* mutant gradually became yellow under regimen 6 (Figure 1C), while the leaves gradually turned green under regimen 9 (Figure 1F). The green leaves did not convert to yellow–green crossbands under regimen 10 (Figure 1G). These observations indicate that light and temperature affected the banding of the *zb7* mutant. Constant low temperature kept the seedlings completely green, while constant light and high temperature can make the plant turn completely yellow.

According to several previous studies, the variegation mutants usually develop nearly normal green leaves under low-light conditions. However, under middle or high intense light, the yellow/white sectors are enlarged or even necrotic. Reduced PSII activity and accumulation of ROS are generally observed in the damaged leaf cells (Fang et al., 2008; Rosso et al., 2009; Li et al., 2010). To examine this possibility, we grew *zb7* and wild-type plants at 25°C but under different lighting conditions from 5 μmol photons m^{-2} s^{-1}, 250 μmol photons m^{-2} s^{-1} to 400 μmol photons m^{-2} s^{-1}. As shown in Figure 2, the zebra phenotype of all *zb7* mutants did not revert under low-light conditions; instead, they turned enhanced yellow

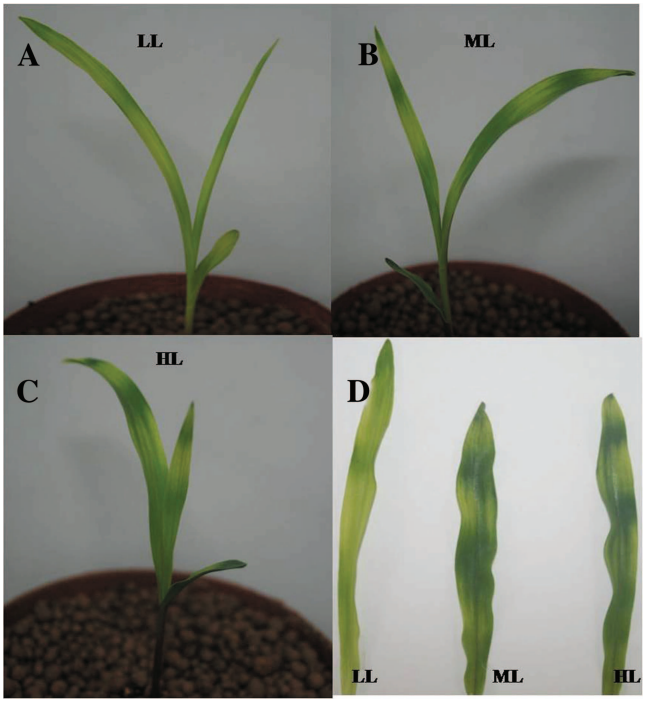

Figure 2. Phenotype of *zb7* Mutant Grown under Different Light Intensity.

Seeds from both the wild-type and *zb7* were grown at 25°C in growth chambers under three different light conditions.

(A–C) Representative photographs of *zb7* mutants grown at 5, 250, and 400 μmol photons m^{-2} s^{-1} light intensity.

(D) The phenotype of the third leaves of *zb7* mutants from different light growth conditions were compared. LL, ML, and HL represent low-light (5 μmol photons m^{-2} s^{-1}), moderate-light (250 μmol photons m^{-2} s^{-1}), and high-light (400 μmol photons m^{-2} s^{-1}) conditions, respectively.

(Figure 2A and 2D). And the high-light condition did not enlarge the yellow section either (Figure 2B–2D). We also measured the maximal photochemical efficiency of PSII (variable fluorescence F_v/maximum fluorescence F_m) to assess the PSII function of the mutant. F_v/F_m practically shows the potential yield of PSII photochemistry and is approximately 0.83 for a wide variety of plants (Horton and Bowyer, 1990). Under the three different light conditions, the F_v/F_m values of both the *zb7*-G and *zb7*-Y were lower than the wild-type, while F_v/F_m values of *zb7*-Y were only 63–80% of wild-type (Table 2). Under low-light conditions (5 μmol photons m^{-2} s^{-1}), the F_v/F_m values of *zb7*-Y did not increase. Under high-light conditions (400 μmol photons m^{-2} s^{-1}), it also did not drop. These results suggested that a proportion PSII reaction centers were damaged, but the zebra phenotype and the arrest of chloroplast development in *zb7* mutants are not due to the secondary effect of photooxidative stress.

Genetic Analysis and Fine Mapping of *zb7*

To genetically analyze the *zb7* mutant, the homozygous *zb7* mutant plants were crossed with B73, Mo17, and Zong31, respectively. The phenotypes of all the F_1 plants were the same as that of the wild-type. Three backcross populations were constructed from crosses between the *zb7* mutant and B73, Mo17, and Zong31. The phenotypes showed a segregation ratio of 1:1 (zebra plants: green plants, $x^2 < x^2_{0.05} = 3.84$; $P > 0.05$; Supplemental Table 1) in each backcross population. Thus, the leaf phenotype of the *zb7* mutant is controlled by a single-recessive nuclear gene.

The *zb7* locus had been mapped to the long arm of maize chromosome 1 (Neuffer MG, 1987; Sisco, 1988). To validate this mapping position, a BC1 population was generated from a cross between the *zb7* mutant and B73. Initial mapping revealed that the *zb7* was located in a 4.2-Mb region between simple sequence repeat (SSR) markers umc2189 and umc1534 (Figure 3A). To further refine the position of *zb7*, a large population was examined, including 6500 plants from the BC1 segregation population and 968 plants exhibiting the zebra crossbands from the F_2 segregation population. Based on the genome sequence of B73 (archive.maizesequence.org), six SSR markers and four cleaved–amplified polymorphic sequences (CAPS) were developed between umc2189 and umc1534 (Supplemental Table 2). According to the genotypes and phenotypes of the recombinants, *zb7* was eventually mapped to a 160-kb region between CAPS1 and AC209801SSR located on BAC AC211483 and AC209801, respectively (Figure 3B and 3C).

zb7 Encodes IspH, an IPP/DMAPP Synthase

Further analysis of the region led to the identification of a putative gene that encoded the IspH (LytB or HDR) protein, which functions in chloroplast development and has high sequence homology with the *A. thaliana* IPP/DMAPP synthase gene. The IspH catalyzes the reaction of HMBPP to IPP and DMAPP in the last step of the MEP pathway. As a candidate gene, the open

Table 2. Chlorophyll Fluorescence Parameters in the Wild-Type and Mutant Plants under Different Light Intensity.

	Low-light intensity			Moderate-light intensity			High-light intensity		
Parameter	Wild-type	*zb7*-G	*zb7*-Y	Wild-type	*zb7*-G	*zb7*-Y	Wild-type	*zb7*-G	*zb7*-Y
F_0	0.23 ± 0.02	0.27 ± 0.05	0.45 ± 0.02	0.25 ± 0.01	0.23 ± 0.01	0.32 ± 0.01	0.22 ± 0.01	0.25 ± 0.03	0.34 ± 0.02
F_m	1.20 ± 0.12	0.99 ± 0.13	0.91 ± 0.04	1.32 ± 0.10	1.00 ± 0.06	0.91 ± 0.08	1.22 ± 0.03	1.03 ± 0.08	0.98 ± 0.08
F_v/F_m	0.81 ± 0.01	0.73 ± 0.02	0.51 ± 0.01	0.81 ± 0.04	0.77 ± 0.01	0.65 ± 0.02	0.82 ± 0.03	0.76 ± 0.02	0.65 ± 0.03

The F_0 and F_m values were measured in fully matured third leaf blades of three-leaf-old plants raised in growth chambers. Mean and SD values were obtained from five measures. *zb7-G* and *zb7*-Y represent the green and yellow sectors of the mutant, respectively.

reading frame (ORF) was amplified from the *zb7* mutant and wild-type by reverse transcription polymerase chain reaction (RT–PCR). Sequencing and comparison of the RT–PCR products indicated that the recessive *zb7* has a single nucleotide alteration at codon 190 (C to T) in the first exon, which resulted in an amino acid change at residue 64 from Arg to Cys (Figure 4A). Analyses of 10 maize inbred lines by sequencing and restriction enzyme digestion (MaeI) revealed that this nucleotide substitution is specific in the *zb7* mutant (data not shown). Therefore, we conclude that *zb7* corresponds to *IspH* gene.

Zb7 is a single copy gene in maize genome with a 1389-bp ORF. The ORF of the *Zb7* gene includes 10 exons and encodes a 462 amino acid protein named IspH (LytB or HDR) that has a molecular mass of ~51.6 kD. HDR is a chloroplast protein with an apparent chloroplast-targeting region of 35 amino acids at its N-terminus according to the ChloroP algorithm (Emanuelsson et al., 1999). HDR is located in the stroma of the chloroplast (Guevara-García et al., 2005). Sequence alignments of multiple amino acid sequences from different organisms revealed that the IspH (LytB or HDR) of maize shared high homology with proteins from other plants, including that from *Cyanobium s*p. (61%) and *E. coli* (21%) (Figure 4C). There is 76–93% sequence identity between IspH proteins of maize and those of various higher plant species, such as *Sorghum* (93%), *Oryza sativa* (88%), *C. acuminata* (80%), *Hevea brasiliensis* (79%), *Arabidopsis* (77%), and *A. annua* (76%) (McAteer et al., 2001; Guevara-García et al., 2005; Kim et al., 2008; Sando et al., 2008; Wang et al., 2008) (Figure 4C). There are four conserved cysteine residues in the IspH protein of plant and *Cyanobium* sp., but the conserved cysteine residues are missing in that of *Synechococcus* and *E. coli*. The non-conserved cysteine residues in *E. coli* might participate in the coordination of the iron–sulfur bridge proposed to be involved in the catalytic center (Seemann et al., 2002; Wolff et al., 2003). Phylogenetic analysis using sequences of IspH protein from various species revealed that maize IspH cluster together with that of *Sorghum* and rice, and is more distantly related to the proteins from *C. acuminata*, *H. brasiliensis*, *A. thaliana*, *A. annua* and *Nicotiana tabacum* (Figure 4B).

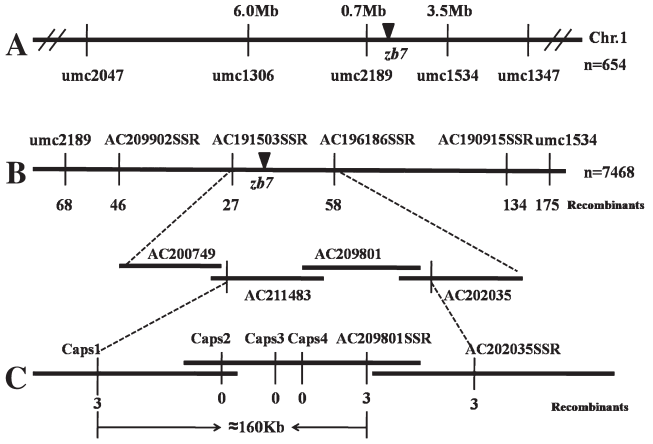

Figure 3. Map-Based Cloning of the *zb7* Gene.

The map was constructed based on the publicly available sequence of maize chromosome 1. Five SSR markers (umc2047, umc1306, umc2189, umc1534, bnlg1347) were obtained from the public database on Maize GDB; six SSR markers (AC209902, AC191530, AC196186, AC190915, AC202035SSR, AC209801SSR) and four CAPS markers (CAPS1, CAPS2, CAPS3, CAPS4) were developed using SSR Hunter software and sequences based on the B73 genome. Numbers indicate recombinants at the marker regions.

(A) The *zb7* locus was mapped to an interval between markers umc2189 and umc1534 at the long arm of maize chromosome 1 (Chr.1) using 654 BC_1 segregation individuals.

(B) Fine mapping of the *zb7* locus. The locus was delimited between AC191530 and AC196186 using 6500 segregation populations of BC_1 and 968 recessive individuals of F_2; four BAC contigs (AC200749, AC211483, AC209801, AC202035) cover the *zb7* 1ocus.

(C) The *zb7* gene was narrowed down to a ~160-kb genomic DNA region between the CAPS marker CAPS1 and SSR marker AC209801SSR, and co-segregated with CAPS2, CAPS3, and CAPS4.

Gene Silencing of IspH Results in an Albino Phenotype

The function of IspH has been investigated in *Nicotiana benthamiana*. TRV-IspH-induced gene silencing caused an albino phenotype that reduced chlorophyll and carotenoid pigments to less than 4% of normal levels (Page et al., 2004). A single nucleotide insertion in the eighth exon of IspH caused a premature translation termination in the *clb6* mutant of *A. thaliana* that resulted in an albino phenotype (Guevara-García et al., 2005). An *A. thaliana* IspH null mutant (owing to T-DNA insertion) has an albino phenotype and transgenic lines of *Arabidopsis* that are caused by IspH transgene-induced gene silencing showing various albino patterns (Hsieh and Goodman, 2005). All previous research on the *IspH* gene implied that it plays an indispensable role

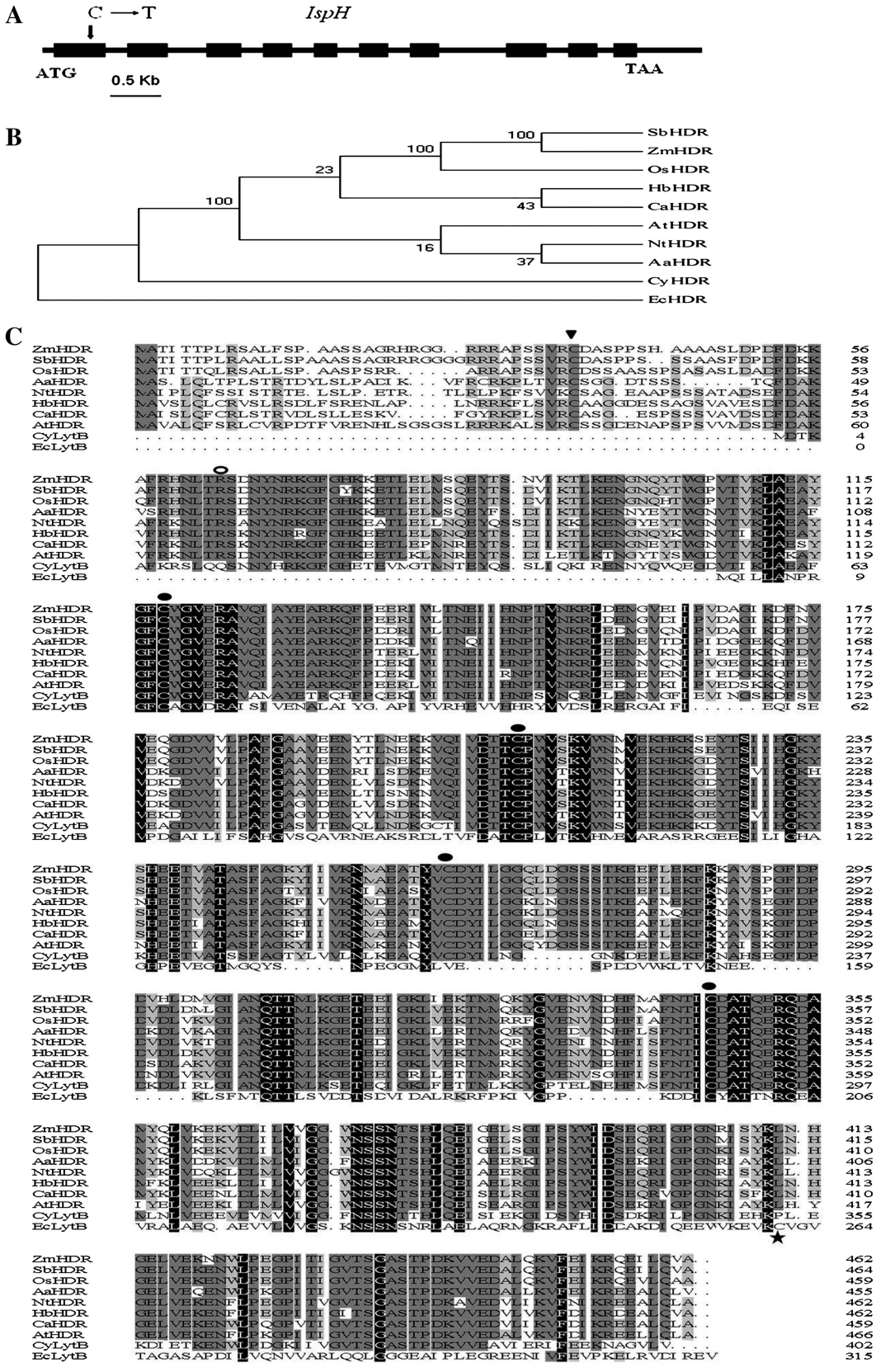

Figure 4. Structure of *IspH* Gene and Sequence Alignment of Multiple Amino Acids from Different Organisms and Analysis of Phylogenetic Tree.

in the early stages of chloroplast development. To confirm the function of maize *IspH* gene, an anti-sense vector of 35S: IspH cDNA was constructed in order to silence the *IspH* gene. Transgenic maize plants showed complete albino (Figure 5C). The anti-sense sequence of *IspH* was only detected in the albino plants, while this was not detected in the transgenic plants with empty vector, which shows a normal phenotype (Figure 5A), suggesting that albino plants were causing by the silencing of the *IspH* gene. Total RNA of albino tissue was extracted for RT–PCR analysis of *IspH* expression. There was no *IspH* expression in the albino tissue (Figure 5B). The contents of chlorophylls and carotenoids were normal in the empty vector transgenic plants, while there was a huge reduction in the levels of these pigments (close to zero) in albino tissues. There were no chloroplasts in the cells from the albino tissues (Figure 5D). Transgenic albino plants gradually died after 2 weeks. This suggests that *IspH* is essential in maize during the early stages of chloroplast development.

Photoperiod-Regulated Expression of IspH and the Increased mRNA Accumulation in the Leaves of Late Development Stages of *zb7* Plants

To assess the temporal and spatial expression of *IspH*, total RNA was extracted from wild-type and *zb7* mutant plants in different developmental stages. The results of RT–PCR showed that *IspH* was expressed in various tissues (stems, leaves, ears, and tassels) at levels that did not differ significantly from each other. The expression was lower in the roots in both wild-type and *zb7* mutant plants (Figure 6A). While under conditions of 48-h light/48-h dark and 48 h at 32°C/48 h at 20°C, the expression level of *IspH* was detected to remain unchanged (Figure 6B).

To further investigate whether the expression of *IspH* gene is modulated by photoperiod, we compared the day/night expression patterns during the 16-h light/8-h dark photoperiod conditions. Test samples were taken every 2 h. qRT–PCR showed the expression of *IspH* oscillated during a light/dark cycle. Higher transcript levels were detected during earlier light period and later dark period (Figure 6C).

The *zb7* mutant developed transverse-striped leaves with yellow–green sectors in its seedling stage, the yellow–green crossbands gradually disappeared with the growth of the mutant. To explore the possible reason for the restoration of green color in later stages of growth, we detected the expression of *IspH* and other genes involved in the MEP pathway at different stages between *zb7* mutant and wild-type. RT–PCR showed that *IspH* mRNA was expressed more abundantly after the six-leaf stage compared with the three-leaf stage of *zb7*; the expression level was even higher than the wild-type. The other genes involved in the MEP pathway shared similar expression pattern except *IspG* (Figure 6D). The higher expression level at late development stages of *zb7* might be a possible reason for the restoration of green.

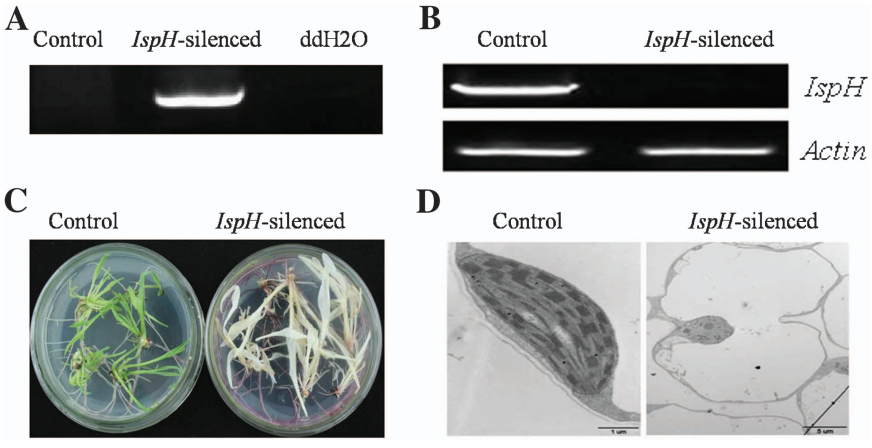

Figure 5. Maize 35S:*IspH* cDNA Transgene-Induced Gene Silencing.
The cDNA fragment was 470 bp from CDS-582 to CDS-1052 and the reverse cDNA fragment contained BglII and BstEII restriction enzyme sites and a GC protective base.
(A) Detection of IspH DNA.
(B) RT–PCR analysis of *IspH* in wild-type and *IspH* gene silencing line. The maize actin was used as a control.
(C) The wild-type control and the transgene albino plant that was IspH-silenced.
(D) Chloroplast ultrastructure of control and transgene albino plants that was IspH-silenced.

(A) Schematic diagram of *IspH* gene ORF with mutation from C to T.
(B) Multiple alignments of HDR sequences from the gene bank published on NCBI for maize (Zm, cl00507), *Sorghum* (Sb, SORBIDRAFT_01g009140), rice (Os, OsI_13396), *Artemisia* (Aa, ABY57296), *Nicotiana* (Nt, AAD55762), *Hevea* (Hb, BAF98297), *Camptotheca acuminata* (Ca, ABI64152), *Arabidopsis* (At, AT4G34350), *Cyanobium* sp. (Cy, ATCC 51142), and *Escherichia coli* (Ec, P22565). Identical residues are boxed in black; similar residues are highlighted in gray. The triangle indicates the position of the cleavage site of the plastid-targeting peptides predicted with the ChloroP algorithm. Four conserved cysteine residues are denoted by solid dots. The Arg to Cys mutation at position 64 is indicated by an empty dot. The non-conserved cysteine residues in *E. coli* are indicated with asterisks.
(C) A phylogenetic tree of HDR from different organisms generated with MEGA.2.0.

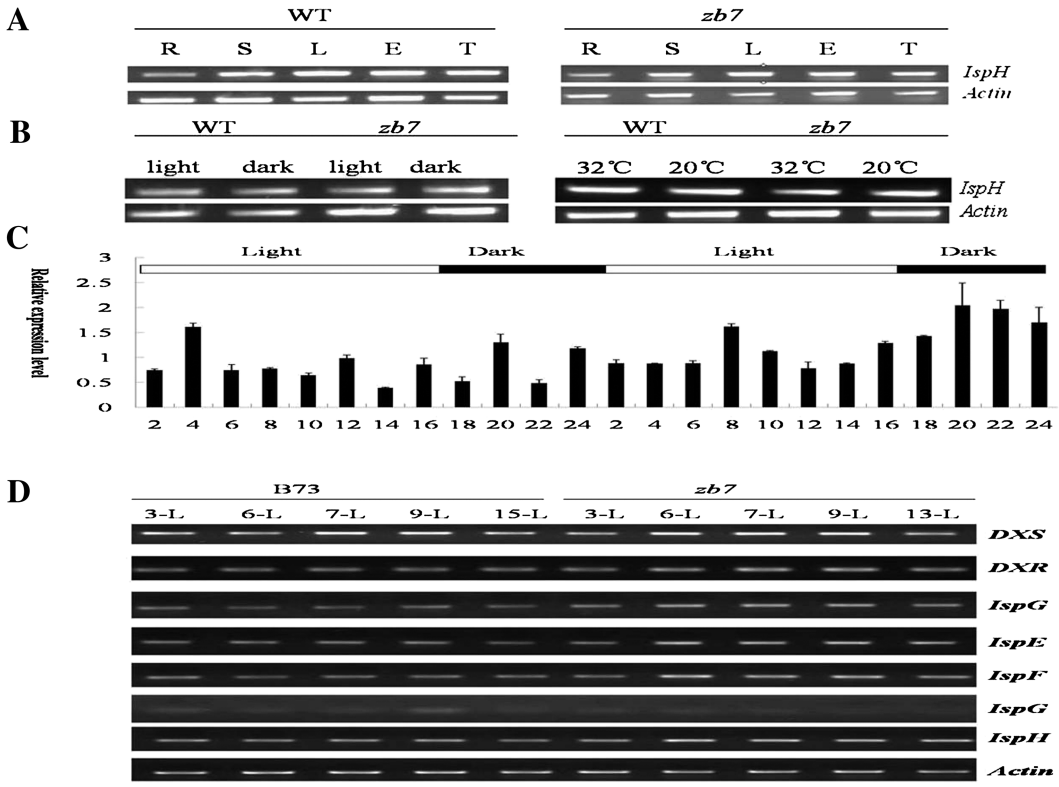

Figure 6. Expression of *IspH* by RT–PCR.

(A) Expression of *IspH* in root (R), stalk (S), leaf (L), ear (E), and tassel (T) of wild-type and *zb7* mutant plants.

(B) *IspH* expression in wild-type and *zb7* mutant three-leaf plants grown in 48-h light or 48-h dark and 48 h at 32°C or 48 h at 20°C.

(C) Expression pattern of *IspH* in a normal 16-h light/8-h dark cycle at 2 d; samples were collected every 2 h.

(D) Expression of MEP genes between wild-type and mutant plants at different developmental stages: three-leaf stage (3-L), six-leaf stage (6-L), seven-leaf stage (7-L), nine-leaf stage (9-L), 13-leaf stage (13-L), 15-leaf stage (15-L).

DISSCUSION

Zb7 Encodes 1-hydroxy-2-methyl-2-(E)-butenyl-4-diphosphate (HMBPP) Reductase in Maize

In this study, we cloned the *zb7* gene by a map-based cloning strategy. Our result indicates that *zb7* encodes the IspH protein of the plastid MEP pathway. Levels of chlorophylls and carotenoids were significantly reduced in the *zb7*-yellow section compared with the *zb7*-green and wild-type plants at the three-to-four-leaf stage, but they increased gradually to the same level as the wild-type at adult stage (Table 1). The simultaneous increase in chlorophyll and carotenoid contents (with associated phenotypic changes) indicated that mutation of IspH affected the syntheses of chlorophyll and carotenoid in parallel. In the *zb7*-yellow cells, the biosynthesis of the photosynthetic apparatus was affected detrimentally with incomplete thylakoid performance and vesicle structures of high electron density (Figure 1J and 1K); however, the chloroplasts gradually developed into normal chloroplasts at more mature stages of development. Interestingly, although the intergranal lamella layers in the *zb7*-green plants were thinner and fewer than in the wild-type (Figure 1I), the contents of chlorophylls and carotenoids were the same as in wild-type (Table 1), suggesting that the impaired chloroplasts in the *zb7*-green plants were sufficient for syntheses of these pigments.

Sequence comparison of IspH cDNA between *zb7* mutant and wild-type plants revealed that a single nucleotide change (C to T) in the highly conserved region resulted in an amino acid alteration (Arg to Cys). This alteration might affect the stability and activity of the IspH. The GcpE and IspH/LytB of *E. coli* and GcpE of *A. thaliana* of the MEP pathway are all diphosphate reductases belonging to the $[4Fe–4S]^{2+}$ protein family (Seemann et al., 2002; Wolff et al., 2003; Seemann et al., 2005). The enzyme catalytic center requires a double one-electron transfer involving the $[4Fe–4S]^{2+}$ cluster. At the active site, there is the $[4Fe–4S]^{2+}$ cluster and a redox-active disulfide bridge, which contains four conserved cysteine residues that are linked to the sulfur via a disulfide bond. The LytB protein of *E. coli* has only three conserved cysteines (at positions 12, 96, and 197) but these are essential for binding the iron–sulfur center to apoprotein. The non-conserved cysteine at position 261 might participate in $[4Fe–4S]^{2+}$ coordination, and the $[4Fe–4S]^{2+}$ center has been shown to have unusual coordination using *in vivo* Mossbauer Spectroscopy (Seemann

et al., 2002, 2005, 2009). Amino acid sequence alignment from different organisms suggested that the IspH is highly conserved, although there is only ~21% identity between the *Zea mays* and *E. coli* proteins (Figure 4C). There are four conserved cysteine residues in the amino acid sequences of IspH from plants and *Cyanobium* sp. and a highly conserved region at the N-terminus that is absent from the *E. coli* protein. This result suggests a similar enzymatic mechanism for LytB in plants and *Cyanobium* sp. The conserved cysteine residues and N-terminus sequence can play important roles for the activity or the stability of the IspH protein. Thus, it is hypothesized that the mutation of the conserved amino acid at position 64 in the *zb7* mutant might affect the enzyme activity or stability.

In *E. coli*, LytB catalyzes HMBPP to IPP and DMAPP in a ratio of ~5.5:1 in the last step of the MEP pathway (Altincicek et al., 2001; Adam et al., 2002; Rohdich et al., 2002, 2003). Mutation of IspH in *E. coli*, *cyanobacteria*, and *A. thaliana* confirmed the role of this enzyme in isoprenoid biosynthesis via the MEP pathway (Cunningham Jr et al., 2000; Altincicek et al., 2001; McAteer et al., 2001; Guevara-García et al., 2005; Hsieh and Goodman, 2005). In *IspH*-silencing of maize, no expression was detected (Figure 5B), while the cell contents of chlorophylls and carotenoids were close to zero. In addition, the chloroplasts were almost without thylakoids and contained large vesicle structures (Figure 5D). Thus, these observations are similar to those seen in *N. benthamiana* and *A. thaliana*, where loss of function and gene silencing of IspH produced an albino phenotype with impaired chloroplasts containing large vesicles. In plants, the chlorophylls and carotenoids are synthesized in the chloroplast, and play important roles in photosynthesis and protecting the photosynthetic apparatus; as such, it was not surprising at all that the IspH-silenced maize plants died gradually up to 2 weeks of age.

Possible Mechanism of the Transverse Yellow–Green Phenotype

Zebra is a special kind of chlorophyll-deficient phenotype in plants. In crops, several zebra mutants have been described and some of them have been cloned (Neuffer MG, 1987; Sanchez and Khush, 1992; Huang et al., 2009; Wang et al., 2009; Li et al., 2010; Chai et al., 2011). A fundamental question is how the zebra bands form under the same genetic background. *ZEBRA2* in rice encoding carotenoid isomerase had decreased contents of carotenoids, a group of well-known photoprotective pigments, leading to lower efficiency in scavenging ROS in the PS II followed by the accumulation of ROS that results in photoinhibition and photobleaching (Fang et al., 2008; Chai et al., 2011). Mutation on rice *ZN* gene had caused decreased PSII recovery rates, resulting in the accumulation of ROS and hypersensitive to photoinhibition. In our research, the *zb7* mutant was affected by light and temperature. Plants grown at lower temperatures (below 22°C) were shown to be completely green, while constant light and constant high temperatures produced completely yellow plants. Unlike other previously reported zebra mutants, intensity of light does not obviously affect the zb7 phenotype. Under low light intensity, the zebra phenotype of all *zb7* mutants did not revert (Figure 2A and 2D). And the high-light condition did not enlarge the yellow section either (Figure 2B–2D). Our data suggest that the damage of the PSII is not the direct cause of the zebra phenotype—a result that is consistent with a previous study of *clb* mutans in *Arabidopsis* (Gutiérrez-Nava et al., 2004).

IspH is constitutively expressed lower in the roots, but highly expressed in stem, mature leaves, ear, and tassel during flowering (Figure 6A). The expression of all MEP pathway genes is highly expressed in the light but only expressed at low levels in the dark, with the exception of *IspH*, which is also coordinately regulated by a 16-h light/8-h dark photoperiod. The single nucleotide mutation in *zb7* did not affect the expression of *IspH* in maize. qRT–PCR results from 16-h light/8-h dark conditions showed the highest expression of IspH in the early light and late dark periods (Figure 6C). These observations are consistent with a previous study in *Arabidopsis* (Hsieh and Goodman, 2005). The *zb7* mutant still exhibited the zebra phenotype under constant light and the 16-h at 32°C/8-h at 22°C regimen, suggesting that temperature might affect the enzyme activity of IspH. Therefore, it is hypothesized that, under low-temperature (below 22°C) conditions, IspH enzyme activity is more stable and the syntheses of chlorophylls and carotenoids are the same as the wild-type, although different expression levels are observed during a single day. Under constant high temperatures (higher than 22°C), enzyme activity is reduced or partially deactivated, and the photoperiod is important for the exhibition of the diurnal crossbands. Under constant light, different temperatures result in distinct enzyme activity and this is the key for the expression of the phenotype. Constant light and higher temperatures (32°C) result in lower *IspH* expression and reduced enzyme activity, causing a completely yellow phenotype. In conclusion, our results suggest that the less effective or unstable IspH in *zb7* mutant and the diurnal expression of IspH together accounted for the zebra phenotype under normal growth conditions.

Restoration of Green Related to the Higher Expression Level at Late Development Stages of *zb7*

Mutation of *IspH* resulted in a diurnal transverse yellow–green phenotype more or less specific to younger leaves. The reason for the restoration of green color in later stages is not fully understood. It is possible that there is functional redundancy resulting from another gene that functions in a similar manner to *IspH*. Genes in the MEP pathway in plants were thought to exist almost entirely in a single copy, with the exception of *DXS* in *Arabidopsis* and rice. Moreover, studies on *C. acuminata* showed that *CaHDR* belonged to a low-copy gene family, but a multicopy phenomenon for HMBPP reductase was found in gymnosperms *Ginkgo biloba* and *Pinus taeda* (Botella Pavía et al., 2004; Kim et al., 2008; Wang et al., 2008). BlastN searches of the *IspH* gene in the maize genome indicated that *IspH* is

a single copy gene, which is consistent with the HDR in angiosperms. IPP and DMAPP are synthesized in the MVA and MEP pathways, and crosstalk between cytosolic and plastidial pathways has been reported previously in plants. Indeed, IPP and DMAPP is transported unidirectionally from plastids to cytosol in spinach, and it is the MVA-derived products that contribute to the formation of chlorophylls and carotenoids needed for plastid development (Eisenreich et al., 1998; Lichtenthaler, 1999; Eisenreich et al., 2001; Kasahara et al., 2002; Nagata et al., 2002; Rodríguez-Concepción and Boronat, 2002; Bick and Lange, 2003; Laule et al., 2003; Rohmer, 2003). *IspH*-silencing in *Arabidopsis* and maize resulted in a lethal albino phenotype, suggesting that there is no or little cytosolic IPP and DMAPP transported into the plastids or chloroplasts and this is insufficient for survival in the seedling stage. Whether such transportation occurs in later developmental stages is unknown. Expression of *IspH* in the *zb7* mutant is higher than wild-type in later stages (Figure 6D), and this might explain the restoration of the green phenotype in these plants. The elevated expression of *IspH* in *zb7* mutant of the later stages could be due to the feedback regulation of the MEP pathways. Posttranscriptional regulation modulates the expression levels of *IspH* and other genes in the MEP pathway had also been suggested before (Botella Pavía et al., 2004; Guevara-García et al., 2005; Hsieh and Goodman, 2005; Wang et al., 2008).

METHODS

Plant Materials and Growth Conditions

The *zb7* mutant of maize (*Zea mays*) is an EMS-induced recessive mutant isolated originally by M.G. Nurfeer. It was grown in the Shang Zhuang Experimental Station of the China Agricultural University for phenotype observations. The *zb7* mutant was crossed with B73 to construct the BC_1 mapping population. For light/temperature shift experiments, the *zb7* mutant was grown in illumination incubators at 10 different light and temperature regimens. To assess the potential influence of light intensity on the phenotype, mutant plants were grown at 25°C under three different illumination conditions (5, 250, and 400 μmol photons m^{-2} s^{-1}).

Measurement of Photosynthetic Pigments

Fresh leaf tissue (0.2 g) was taken in triplicate from *zb7* mutant and wild-type plants. Pigments were extracted using 95% ethanol. Chl a, Chl b, and carotenoid levels were determined with a UV/VIS spectrophotometer measuring absorbencies at 665, 649, and 470 nm, respectively. Pigment contents were calculated according to a previously reported method (Lichtenthaler, 1987).

Measurement of Chl Fluorescence

Chlorophyll fluorescence measurements were carried out using a PAM 2100 portable fluorometer (Walz, www.walz.com/) at room temperature. Samples were dark-adapted for 20 min prior to all measurements. The maximum quantum yield of PSII photochemistry, F_v/F_m, was calculated as $F_v/F_m = (F_m - F_0)/F_m$ (Genty et al., 1989).

Transmission Electron Microscopy

Leaf samples of *zb7*-green, *zb7*-yellow, and B73 at different stages of development were fixed in 4% glutaraldehyde (0.2 M phosphate buffer; pH 7.2) for 16 h at 4°C, and then further fixed in 1% osmium tetroxide for 6 h at 4°C. The samples were passed through a series of alcohol solutions and then embedded in Spurr resin. The dehydrated samples were cut on a Reichert Ultracut-S and viewed with a transmission electron microscope (JEOL 100 CX).

Marker Development and Fine Mapping

The fine mapping population included 6500 BC_1 and 968 F_2 segregation plants and was constructed by crossing the *zb7* mutant and B73. Genomic DNA was extracted and analyzed for cosegregation using available SSR markers (www.maizegdb.org). New SSR markers were found using the SSRHunter 1.3 Simple Sequence Repeat Search tool and designed using Primer 5.0 based on the B73 genome sequence (www.maizesequence.org). CAPS markers were developed using SNP2CAPS software on sequence comparisons between the *zb7* mutant and B73 according to the published sequence of B73 (www.ncbi.nlm.nih.gov).

Sequence Analyses

IspH amino acid sequences from different organisms were acquired from the National Center for Biotechnology Information database and used for phylogenetic analyses. The plastid-targeting peptide was predicted with SignalP version 3.0 (Emanuelsson et al., 2007). Multiple amino acid sequence alignments and phylogenetic analyses were performed using DNAMAN version 6.0 (Lynnon Biosoft).

Construction of Anti-Sense Vector for *IspH* and Maize Transformation

Total RNA was extracted from B73 at the three-leaf stage for RT–PCR and part of the IspH full-length cDNA amplified using primers 5′-GCGGTAACCTACACGCTAAATGAGAAGAAGGT-3′ and 5′-GCAGATCTTCCTGAGTGGCATCACAAAT-3′. The PCR product was cloned into pEASY-T1 cloning vector for sequencing and plasmid was extracted using the Easy Pure Quick Gel extraction kit (Transgen Biotech). Then, the plasmid was digested using two restriction enzymes (*Bgl*II and *Bst*EII). The fragment was recovered using a QiA Quick Gel extraction kit. The fragment of IspH cDNA was subcloned into the plant expression vector pCAM 3301, and transformed into immature embryos according to an agrobacterium-mediated transformation method.

Maize immature embryos dissected at 12 days after pollination(DAP), explanted on N6E medium, and incubated in the dark for 2 or 3 d. Explanted embryos were immersed in 1–1.5 ml of *A. tumefaciens* suspension. The infection was accomplished by gently inverting the tube 20 times before resting it upright

for 5 min with embryos submerged. After infection, embryos were transferred to the surface of co-cultivation medium and incubated in the dark at 20 or 23°C for 3 d. After 4–7 d on resting medium (28°C, dark), embryos were transferred to selection medium (30 per plate) containing 1.5 mg l^{-1} bialaphos. Selection was increased to 3 mg l^{-1} bialaphos 2 weeks later. Putatively transformed events were identified as early as 5 weeks after infection. Regeneration of R_0 transgenic plants from Type II embryogenic callus was accomplished by a 2–3-week maturation step on Regeneration Medium I followed by germination in the light on Regeneration Medium II. Stable transformation efficiency (%) was calculated as the number of bialaphos-resistant callus events recovered per 100 embryos infected. The transgene plants were detected using primers 5′-GAAGGTGGCTCCTACAAA-3′ and 5′-AACCCATCTCATAAA TAACG-3′.

Analysis of RT–PCR and qRT–PCR

According to the method by Wadsworth et al. (1998), total RNA from different organisms, leaves of plants in different developmental stages, and distinct light or temperature regimens were extracted for reverse transcription. First, RNA was digested by DNaseI for 40 min at 37°C; then, the reaction was stopped with stop solution by incubation at 65°C for 10 min. RNA was reverse-transcribed into cDNA using oligo and avian myeloblastosis virus reverse transcriptase. For semiquantitative qRT–PCR, actin primers were used as control (5′-TCACCCTGTGCTGCTGACCG-3′ and 5′-GAACCGTGTGGCTCACACCA-3′). Expression analyses of *zb7* mutant and wild-type was carried out using specific primers (5′-GCATCTGGCTCACCAACGAA-3′ and 5′-GCTCCAAATGCAGGCAACAC-3′). Levels of gene expression in the MEP pathway were analyzed by qRT–PCR for *DXS*, *DXR* (*IspC*), *IspD*, *IspE*, *IspF*, *IspG*, *IspH* of maize using the following primers: *DXS* 5′-AGGACTCCCATTTCGCTTCG-3′ and 5′-TCATGTGGACGGGGTAGTTGA-3′; *DXR* 5′-AGAAGTTGCTCGCCATCCAG-3′ and 5′-TTGCCAATGCTATGTCTTTACC-3′; *IspD* 5′-AGTCAAAGAAGTCGTGGTGG-3′ and 5′-ACTAAGGGCCTTGCAGAAT-3′; *IspE* 5′-CCAACTGGTGCTGGTCTTG-3′ and 5′-ATGCTGCTCCTCGTGAAAA-3′; *IspF* 5′-TTAGCCCGTTCAAGGAGACAATC-3′ and 5′-CGCATCAGGAGAACTACGGTATGA-3′; *IspG* 5′-TTGGAGCAAGTTGAAAGATGTG-3′ and 5′-TTGGAGCAAGTTGAAAGATGTG-3′; and *IspH* 5′-GCATCTGGCTCACCAACGAA-3′ and 5′-GCTCCAAATGCAGGCAACAC-3′. Photoperiod expression of *IspH* was detected by qRT–PCR using primers 5′-GCATCTGGCTCACCAACGAA-3′ and 5′-GCTCCAAATGCAGGCAACAC-3′. Tubulin was selected as the control using primers 5′-TCACCCTGTGCTGCTGACCG-3′ and 5′-GAACCGTGTGGCTCACACCA-3′. The reaction volume was 30 μl and included 0.5 μM of each primer and 1XSYBR Green PCR master mix (Takara). The reaction procedure was carried out in a BIO-RAD cycler as follows: 95°C for 10 min, 40 cycles of 95°C for 15 s, 60°C for 15 s, and 72°C for 15 s.

SUPPLEMENTARY DATA

Supplementary Data are available at *Molecular Plant Online.*

FUNDING

This work was supported by the National Basic Research Program of China (973 Program) (2009CB118400) and National High-tech R&D Program (863 Program) (2010AA10A106). No conflict of interest declared.

REFERENCES

Adam, P., et al. (2002). Biosynthesis of terpenes: studies on 1-hydroxy-2-methyl-2-(E)-butenyl 4-diphosphate reductase. Proc. Natl Acad. Sci. U S A. **99,** 12108.

Altincicek, B., et al. (2001). LytB, a novel gene of the 2-C-methyl–erythritol 4-phosphate pathway of isoprenoid biosynthesis in *Escherichia coli*. FEBS Lett. **499,** 37–40.

Aluru, M.R., Bae, H., Wu, D., and Rodermel, S.R. (2001). The *Arabidopsis immutans* mutation affects plastid differentiation and the morphogenesis of white and green sectors in variegated plants. Plant Physiol. **127,** 67–77.

Araki, N., Kusumi, K., Masamoto, K., Niwa, Y., and Iba, K. (2000). Temperature-sensitive *Arabidopsis* mutant defective in 1-deoxy-d-xylulose 5-phosphate synthase within the plastid nonmevalonate pathway of isoprenoid biosynthesis. Physiol. Plant. **108,** 19–24.

Bick, J.A., and Lange, B.M. (2003). Metabolic cross talk between cytosolic and plastidial pathways of isoprenoid biosynthesis: unidirectional transport of intermediates across the chloroplast envelope membrane. Arch. Biochem. Biophys. **415,** 146–154.

Botella Pavía, P., Besumbes, O., Phillips, M.A., Carretero-Paulet, L., Boronat, A., and Rodríguez-Concepción, M. (2004). Regulation of carotenoid biosynthesis in plants: evidence for a key role of hydroxymethylbutenyl diphosphate reductase in controlling the supply of plastidial isoprenoid precursors. Plant J. **40,** 188–199.

Budziszewski, G.J., et al. (2001). *Arabidopsis* genes essential for seedling viability: isolation of insertional mutants and molecular cloning. Genetics. **159,** 1765.

Carol, P., and Kuntz, M. (2001). A plastid terminal oxidase comes to light: implications for carotenoid biosynthesis and chlororespiration. Trends Plant Sci. **6,** 31–36.

Carol, P., et al. (1999). Mutations in the *Arabidopsis* gene IMMUTANS cause a variegated phenotype by inactivating a chloroplast terminal oxidase associated with phytoene desaturation. Plant Cell. **11,** 57–68.

Carretero-Paulet, L., et al. (2002). Expression and molecular analysis of the *Arabidopsis* DXR gene encoding 1-deoxy-d-xylulose 5-phosphate reductoisomerase, the first committed enzyme of the 2-C-methyl-d-erythritol 4-phosphate pathway. Plant Physiol. **129,** 1581.

Chai, C., et al. (2011). ZEBRA2, encoding a carotenoid isomerase, is involved in photoprotection in rice. Plant Mol. Biol. **75,** 211–221.

Cunningham Jr, F.X., Lafond, T.P., and Gantt, E. (2000). Evidence of a role for LytB in the nonmevalonate pathway of isoprenoid biosynthesis. J. Bacteriol. **182,** 5841.

Disch, A., Hemmerlin, A., Bach, T., and Rohmer, M. (1998). Mevalonate-derived isopentenyl diphosphate is the biosynthetic precursor of ubiquinone prenyl side chain in tobacco BY-2 cells. Biochem. J. **331,** 615.

Eisenreich, W., Rohdich, F., and Bacher, A. (2001). Deoxyxylulose phosphate pathway to terpenoids. Trends Plant Sci. **6,** 78–84.

Eisenreich, W., Schwarz, M., Cartayrade, A., Arigoni, D., Zenk, M.H., and Bacher, A. (1998). The deoxyxylulose phosphate pathway of terpenoid biosynthesis in plants and microorganisms. Chem. Biol. **5,** R221–R233.

Emanuelsson, O., Brunak, S., von Heijne, G., and Nielsen, H. (2007). Locating proteins in the cell using TargetP, SignalP and related tools. Nature Protocols. **2,** 953–971.

Emanuelsson, O., Nielsen, H., and Heijne, G.V. (1999). ChloroP, a neural network-based method for predicting chloroplast transit peptides and their cleavage sites. Protein Sci. **8,** 978–984.

Estévez, J.M., et al. (2000). Analysis of the expression of CLA1, a gene that encodes the 1-deoxyxylulose 5-phosphate synthase of the 2-C-methyl-D-erythritol-4-phosphate pathway in *Arabidopsis*. Plant Physiol. **124,** 95.

Fang, J., et al. (2008). Mutations of genes in synthesis of the carotenoid precursors of ABA lead to pre-harvest sprouting and photo-xidation in rice. Plant J. **54,** 177–189.

Genty, B., Briantais, J.M., and Baker, N.R. (1989). The relationship between the quantum yield of photosynthetic electron transport and quenching of chlorophyll fluorescence. Biochimica et Biophysica Acta (BBA)–General Subjects. **990,** 87–92.

Guevara-García, A., San Román, C., Arroyo, A., Cortes, M.E., de la Luz Gutiérrez-Nava, M., and Leon, P. (2005). Characterization of the *Arabidopsis* clb6 mutant illustrates the importance of post-transcriptional regulation of the methyl-D-erythritol 4-phosphate pathway. Plant Cell. **17,** 628.

Gustafson, C.E., Kaul, S., and Ishiguro, E.E. (1993). Identification of the *Escherichia coli* lytB gene, which is involved in penicillin tolerance and control of the stringent response. J. Bacteriol. **175,** 1203.

Gutiérrez-Nava, M.L., Gillmor, C.S., Jiménez, L.F., Guevara-García, A., and León, P. (2004). CHLOROPLAST BIOGENESIS genes act cell and noncell autonomously in early chloroplast development. Plant Physiol. **135,** 471.

Hansson, M., Cough, S., Kannangara, C., and Von Wettstein, D. (1997). Analysis of RNA and enzymes of potential importance for regulation of 5-aminolevulinic acid synthesis in the protochlorophyllide accumulating barley mutant tigrina-d12. Plant Physiol. Biochem. **35,** 827–836.

Hecht, S., et al. (2001). Studies on the nonmevalonate pathway to terpenes: the role of the GcpE (IspG) protein. Proc. Natl Acad. Sci. U S A. **98,** 14837.

Herz, S., et al. (2000). Biosynthesis of terpenoids: YgbB protein converts 4-diphosphocytidyl-2C-methyl-D-erythritol 2-phosphate to 2C-methyl-D-erythritol 2, 4-cyclodiphosphate. Proc. Natl Acad. Sci. U S A. **97,** 2486.

Horton, P., and Bowyer, J. (1990). Chlorophyll fluorescence transients. Methods Plant Biochem. **4,** 259–296.

Hsieh, M.H., and Goodman, H.M. (2005). The *Arabidopsis* IspH homolog is involved in the plastid nonmevalonate pathway of isoprenoid biosynthesis. Plant Physiol. **138,** 641.

Hsieh, M.H., Chang, C.Y., Hsu, S.J., and Chen, J.J. (2008). Chloroplast localization of methylerythritol 4-phosphate pathway enzymes and regulation of mitochondrial genes in ispD and ispE albino mutants in *Arabidopsis*. Plant Mol. Biol. **66,** 663–673.

Huang, M., et al. (2009). Camouflage patterning in maize leaves results from a defect in porphobilinogen deaminase. Mol. Plant. **2,** 773–789.

Kasahara, H., Hanada, A., Kuzuyama, T., Takagi, M., Kamiya, Y., and Yamaguchi, S. (2002). Contribution of the mevalonate and methylerythritol phosphate pathways to the biosynthesis of gibberellins in *Arabidopsis*. J. Biol. Chem. **277,** 45188.

Kim, S.M., Kuzuyama, T., Kobayashi, A., Sando, T., Chang, Y.J., and Kim, S.U. (2008). 1-Hydroxy-2-methyl-2-(E)-butenyl 4-diphosphate reductase (IDS) is encoded by multicopy genes in gymnosperms *Ginkgo biloba* and *Pinus taeda*. Planta. **227,** 287–298.

Kusumi, K., Komori, H., Satoh, H., and Iba, K. (2000). Characterization of a zebra mutant of rice with increased susceptibility to light stress. Plant Cell Physiol. **41,** 158.

Laule, O., et al. (2003). Crosstalk between cytosolic and plastidial pathways of isoprenoid biosynthesis in *Arabidopsis thaliana*. Proc. Natl Acad. Sci. U S A. **100,** 6866.

Li, J., et al. (2010). ZEBRA-ECROSIS, a thylakoid-bound protein, is critical for the photoprotection of developing chloroplasts during early leaf development. Plant J. **62,** 713–725.

Lichtenthaler, H.K. (1987). Chlorophylls and carotenoids: pigments of photosynthetic biomembranes. Methods Enzymol. **148,** 350–382.

Lichtenthaler, H.K. (1999). The 1-deoxy-D-xylulose-5-phosphate pathway of isoprenoid biosynthesis in plants. Annu. Rev. Plant Biol. **50,** 47–65.

Lois, L.M., Campos, N., Putra, S.R., Danielsen, K., Rohmer, M., and Boronat, A. (1998). Cloning and characterization of a gene from *Escherichia coli* encoding a transketolase-like enzyme that catalyzes the synthesis of D-1-deoxyxylulose 5-phosphate, a common precursor for isoprenoid, thiamin, and pyridoxol biosynthesis. Proc. Natl Acad. Sci. U S A. **95,** 2105.

Lüttgen, H., et al. (2000). Biosynthesis of terpenoids: YchB protein of *Escherichia coli* phosphorylates the 2-hydroxy group of 4-diphosphocytidyl-2C-methyl-D-erythritol. Proc. Natl Acad. Sci. U S A. **97,** 1062.

Mandel, M.A., Feldmann, K.A., Herrera-Estrella, L., Rocha-Sosa, M., and León, P. (1996). CLA1, a novel gene required for chloroplast development, is highly conserved in evolution. Plant J. **9,** 649–658.

McAteer, S., Coulson, A., McLennan, N., and Masters, M. (2001). The lytB gene of *Escherichia coli* is essential and specifies a product needed for isoprenoid biosynthesis. J. Bacteriol. **183,** 7403.

Nagata, N., Suzuki, M., Yoshida, S., and Muranaka, T. (2002). Mevalonic acid partially restores chloroplast and etioplast development in *Arabidopsis* lacking the non-mevalonate pathway. Planta. **216,** 345–350.

Neuffer MG, B.J. (1987). Designation of new recessive mutants. MNL. **61,** 50.

Page, J.E., et al. (2004). Functional analysis of the final steps of the 1-deoxy-D-xylulose 5-phosphate (DXP) pathway to isoprenoids in plants using virus-induced gene silencing. Plant Physiol. **134,** 1401.

Rodríguez-Concepción, M., and Boronat, A. (2002). Elucidation of the methylerythritol phosphate pathway for isoprenoid biosynthesis in bacteria and plastids: a metabolic milestone achieved through genomics. Plant Physiol. **130,** 1079.

Rohdich, F., et al. (1999). Cytidine 5′-triphosphate-dependent biosynthesis of isoprenoids: YgbP protein of *Escherichia coli* catalyzes the formation of 4-diphosphocytidyl-2-C-methylerythritol. Proc. Natl Acad. Sci. U S A. **96,** 11758.

Rohdich, F., et al. (2002). Studies on the nonmevalonate terpene biosynthetic pathway: metabolic role of IspH (LytB) protein. Proc. Natl Acad. Sci. U S A. **99,** 1158.

Rohdich, F., et al. (2003). The deoxyxylulose phosphate pathway of isoprenoid biosynthesis: studies on the mechanisms of the reactions catalyzed by IspG and IspH protein. Proc. Natl Acad. Sci. U S A. **100,** 1586.

Rohmer, M. (1999). The discovery of a mevalonate-independent pathway for isoprenoid biosynthesis in bacteria, algae and higher plants. Nat. Prod. Rep. **16,** 565–574.

Rohmer, M. (2003). Mevalonate-independent methylerythritol phosphate pathway for isoprenoid biosynthesis: elucidation and distribution. Pure Appl. Chem. **75,** 375–388.

Rohmer, M., Knani, M., Simonin, P., Sutter, B., and Sahm, H. (1993). Isoprenoid biosynthesis in bacteria: a novel pathway for the early steps leading to isopentenyl diphosphate. Biochem. J. **295,** 517.

Rosso, D., et al. (2009). Photosynthetic redox imbalance governs leaf sectoring in the *Arabidopsis thaliana* variegation mutants immutans, spotty, var1, and var2. Plant Cell. **21,** 3473–3492.

Sanchez, A., and Khush, G. (1992). Seven new genes for zebra character in rice. Rice Genetics Newsletter. **9,** 68–71.

Sando, T., et al. (2008). Cloning and characterization of the 2-C-methyl-D-erythritol 4-phosphate (MEP) pathway genes of a natural-rubber producing plant, *Hevea brasiliensis*. Biosci. Biotechnol. Biochem. **72,** 2903–2917.

Schwender, J., Seemann, M., Lichtenthaler, H., and Rohmer, M. (1996). Biosynthesis of isoprenoids (carotenoids, sterols, prenyl side-chains of chlorophylls and plastoquinone) via a novel pyruvate/glyceraldehyde 3-phosphate non-mevalonate pathway in the green alga *Scenedesmus obliquus*. Biochem. J. **316,** 73.

Seemann, M., et al. (2002). Isoprenoid biosynthesis through the methylerythritol phosphate pathway: the (E)-4-hydroxy-3-methylbut-2-enyl diphosphate synthase (GcpE) is a [4Fe–4S] protein. Angew. Chem. **114,** 4513–4515.

Seemann, M., et al. (2005). Isoprenoid biosynthesis in chloroplasts via the methylerythritol phosphate pathway: the (E)-4-hydroxy-3-methylbut-2-enyl diphosphate synthase (GcpE) from *Arabidopsis thaliana* is a [4Fe–4S] protein. J. Biol. Inorg. Chem. **10,** 131–137.

Seemann, M., et al. (2009). Isoprenoid biosynthesis via the MEP pathway: *in vivo* Mössbauer spectroscopy identifies a $[4Fe\text{-}4S]^{2+}$ center with unusual coordination sphere in the LytB protein. J. Am. Chem. Soc. **131,** 13184–13185.

Sisco, P. (1988). Chromosome 1L mapping of EMS-induced mutants by M.G. Neuffer. MNL. **62,** 124.

Sprenger, G.A., et al. (1997). Identification of a thiamin-dependent synthase in *Escherichia coli* required for the formation of the 1-deoxy-D-xylulose 5-phosphate precursor to isoprenoids, thiamin, and pyridoxol. Proc. Natl Acad. Sci. U S A. **94,** 12857.

Takahashi, S., Kuzuyama, T., Watanabe, H., and Seto, H. (1998). A 1-deoxy-D-xylulose 5-phosphate reductoisomerase catalyzing the formation of 2-C-methyl-D-erythritol 4-phosphate in an alternative nonmevalonate pathway for terpenoid biosynthesis. Proc. Natl Acad. Sci. U S A. **95,** 9879.

Wadsworth, G.J., Redinbaugh, M.G., and Scandalios, J.G. (1988). A Procedure for the small scale isolation of plant RNA suitable for RNA blot analysis. Anal Bio chem. **172,** 279–283.

Wang, Q., et al. (2008). Molecular cloning and characterization of 1-hydroxy-2-methyl-2-(E)-butenyl 4-diphosphate reductase (CaHDR) from *Camptotheca acuminata* and its functional identification in *Escherichia coli*. BMB Rep. **41,** 112–118.

Wang, Q., et al. (2009). Genetic analysis and molecular mapping of a novel gene for zebra mutation in rice (*Oryza sativa* L.). J. Genet. Genom. **36,** 679–684.

Wolff, M., et al. (2003). Isoprenoid biosynthesis via the methylerythritol phosphate pathway: the (E)-4-hydroxy-3-methylbut-2-enyl diphosphate reductase (LytB/IspH) from *Escherichia coli* is a [4Fe-4S] protein. FEBS Lett. **541,** 115–120.

Zeidler, J., Lichtenthaler, H., May, H., and Lichtenthaler, F. (1997). Is isoprene emitted by plants synthesized via the novel isopentenyl pyrophosphate pathway? Zeitschrift fur NaturforschungC Journal of Biosciences. **52,** 15–23.